https://doi.org/10.5194/sp-2024-17
Preprint. Discussion started: 23 September 2024

STATE OF THE PLANET Discussions

Variations of marine heatwaves and cold spells in northwest Atlantic during 1993-2023

Li Zhai[1], Youyu Lu[1], Haiyan Wang[2], Gilles Garric[3], Simon Van Gennip[3]

[1]Fisheries and Oceans Canada, Bedford Institute of Oceanography, 1 Challenger Dr. Dartmouth, NS, B2Y 4A2, Canada
[2]Key Laboratory of Marine Hazards Forecasting, National Marine Environmental Forecasting Center, Ministry of Natural Resources, Beijing, China
[3]Mercator-Ocean International, 2 Av. de l'Aérodrome de Montaudran, 31400 Toulouse, France

Correspondence to: Li Zhai (Li.Zhai@dfo-mpo.gc.ca)

Abstract.

Characteristics of marine heatwaves (MHWs) and cold spells (MCSs) in the northwest Atlantic during 1993-2023 are derived from a global ocean reanalysis product of the EU Copernicus Marine Service. For the surface parameters, the quantification using the reanalysis data is advantageous in regions with the presence of seasonal sea-ice and strong eddies. At the sea bottom, the reanalysis data well reproduces the observed rising trend and sharp increase of bottom temperature around 2012 on Scotian Shelf and associated changes of MHW/MCS parameters. The 31 years of reanalysis data enables the quantification of spatial variations, interannual variations and long-term trends of MHW/MCS parameters in the water column for the first time in our study region.

The corresponding parameters of surface MHWs and MCSs are overall similar due to the nearly symmetrical probability distribution of sea surface temperature (SST) anomalies around the mean. On the Scotian Shelf the MHW parameters and temperature present layered structures in the water column. In the upper layer from surface to a mid-depth interface, the nearly uniform MHW mean intensity of ~2ºC can be mainly attributed to variations of the surface heat flux. From the mid-depth interface to about 130 m depth, the MHW mean intensity has high values of 3-3.5ºC due to the combined effects of downward penetration of upper layer and the lateral advection of water masses. In the deep Emerald Basin below 130 m depth, the MHW intensity has the lowest values of 1.5-2ºC. The MHW frequency has relatively unform values of 1.5-2 per year in the water column, except low values of less than 1 per year below 130 m depth in the Emerald Basin and below 30 m depth over the Emerald Bank. During 1993-2023, the surface MHW (MCS) total days show increasing (decreasing) trends corresponding to the gradual increasing SST, and the MHW total days reached a peak value of 215 days in 2012 corresponding to the highest annual SST. The bottom temperature shows a stronger increasing trend than the SST, and a sharp increase (regime shift) around 2012, resulting in the increasing (decreasing) trend and regime shift of bottom MHW (MCS) total days. In 2012, the bottom MHW total days experienced a sharp increase and the entire water column was warmer than the climatology. The opposite condition presented in 1998 with the longest bottom MCS total days of ~300 near the coast.

https://doi.org/10.5194/sp-2024-17
Preprint. Discussion started: 23 September 2024

The quantification of the extreme conditions in 2012 and 1998 supports the results of previous studies on the impacts of these conditions on several marine life species.

1 Introduction

Marine heatwaves (MHWs) and marine cold spells (MCs) are extreme warm and cold events of the ocean water, respectively. MHWs have been observed in all ocean basins (Collins et al., 2019) and extensively studied. Globally, MHWs, defined relative to a fixed climatological period, have become more frequent, long-lasting, and intense since the 1980s under global warming (Frölicher et al., 2018; Oliver et al., 2018; Fox-Kemper et al., 2021). Regionally, local processes, large-scale climate modes, and teleconnections also play important roles in MHW occurrences (Holbrook et al., 2019; Sen Gupta et al., 2020). In the Northwest Pacific, interannual variations of surface MHWs are correlated with various large-scale atmosphere-ocean indices including the El Niño index (Wang et al., 2024). On the shelf seas of the Northwest Atlantic, nearly half of the surface MHWs are initiated by the positive heat flux anomaly into the ocean, and advection and mixing are the primary drivers for the decay of most MHWs (Schlegel et al., 2021b). On the Newfoundland and Labrador Shelf, the summer and fall MHWs in 2023 were impacted by stratification, winds, and advection (Soontiens et al., 2024). These connections between surface MHWs and physical drivers, thus identified, can be utilized to predict the occurrence of future MHW events.

Previous studies have revealed the negative impacts of MHWs on marine ecosystems. For example, MHWs can cause coral bleaching, destroy kelp forests, and alter the migration patterns of marine species (Santora et al., 2020; Beaudin and Bracco, 2022). MHWs have also affected commercial fisheries in Canadian waters. In the Northeast Pacific, intense and long-lasting heat events, such as “the Blob”, led to fisheries collapses (Free et al., 2023). In Atlantic Canada, extreme heat events affect the physiological behaviour of aquaculture Atlantic Salmon, i.e., the increases of heart rates and decreases of motions (Korus, 2024). The widespread 2012 warm event in the northwest Atlantic, significant in the water column and at sea bottom, had opposite effects on different commercial fisheries. It adversely impacted the snow crab juvenile stages, resulting in a temporary decrease in snow crab abundance on the western Scotian Shelf (Zisserson and Cook, 2017). In the Gulf of Maine, this warm event caused earlier inshore movement of lobsters in the spring, leading to enhanced lobster growth, an extended fishing season, and record landings (Mills et al., 2013).

Compared with MHWs, there have been fewer studies on MCSs. Globally and regionally, the frequency and intensity of surface MCSs show decreasing trends during 1982-2020 associated with the SST increasing (Mohamed et al., 2023; Peal et al., 2023; Schlegel et al., 2021; Wang et al., 2022). Changes in atmospheric forcing, ocean circulation and coastal upwelling can drive local cold events at sea surface (Schlegel et al., 2017) and throughout the water column in shallow coastal bays (Casey et al., 2024).

Studies on surface extreme temperature events commonly use sea surface temperatures (SST) based on satellite remote sensing (e.g., Wang et al., 2022; Peal et al., 2023). Such studies are limited to the upper ocean and ice-free areas, and

https://doi.org/10.5194/sp-2024-17
Preprint. Discussion started: 23 September 2024

the analysis results are impacted by the observational noises, and cloud correction and interpolation schemes used to generate various levels of satellite SST products. Subsurface extreme events have been less well studied due to the scarcity of temperature observations below the surface, leading to limited knowledge about whether and how extreme events at depth have changed over the past decades (Collins et al., 2019). Results from high-resolution numerical ocean models, particularly those reanalysis products achieved through data assimilation, have been alternatively used to study the extreme temperature events, both at surface and at bottom (e.g., Amaya et al., 2023; Wang et al., 2024). The study of Amaya et al. (2023) revealed stronger and longer MHWs at bottom than at surface in the shelf seas of North America, but did not quantify the interannual and long-term variations of MHW characteristics.

Motivated by the results of previous studies, in this study we try to quantify the space-time variations of MHWs and MCSs in Northwest Atlantic, from surface to water column to bottom, with the ultimate goal to better support fisheries in this region. The physical oceanography in the region is quite complex, due to the influences of the strong multi-scale variability of atmospheric forcing, river runoff, the strong ocean circulation of the Gulf Stream, North Atlantic Current and Labrador Current, the meso-scale eddies, etc. (e.g., Loder et al., 1998; Brickman et al., 2018; Ma et al., 2022). Our analysis results will be mainly based on the daily data from an ocean reanalysis product, in comparison with analyses of satellite SST and mooring observations. Main results include 1) characteristics of the spatial distributions of MHW and MCS parameters; 2) the linkages between surface and water column extreme events; and 3) interannual variations and long-term trends, and their relationship with temperature variations and the forcing mechanisms.

2 Datasets and analysis methods

2.1 Datasets

Table 1 lists the datasets analyzed in this study. Product ref. no. 1 is the daily temperature during 1993-2023 from the CMEMS global ocean eddy-resolving reanalysis with a 1/12° horizontal resolution, referred to as GLORYS12v1 (GLORYS), The GLORYS temperature data remains continuous in ice-covered regions, which helps to compensate for the limitations of spatial and temporal coverage of satellite observations in those areas.

Products ref. no. 2 and 3 are global ocean SST analysis produced daily on an operational basis at the Canadian Meteorological Centre (CMC). The analysis incorporates *in situ* observations and retrievals from one microwave and three infrared sensors (Brasnett, 2008). According to the assessment by Fiedler et al., (2019), the CMC SST data show low standard deviations and mean differences to the independent Argo observations, in comparison with other long-term SST analyses including the ESA SST CCI (European Space Agency Sea Surface Temperature Climate Change Initiative) and MyOcean OSTIA (Operational Sea Surface Temperature and Ice Analysis) available from the Copernicus marine catalogues. Product ref. no. 3 at 0.1º resolution during 2017-2023 is linearly interpolated onto the 0.2º grids of product ref. no. 2, thus creating a dataset on unified grids covering 1993-2023. CMC SST has no values at locations and time when sea ice is present.

https://doi.org/10.5194/sp-2024-17
Preprint. Discussion started: 23 September 2024

Product ref. no. 4 is the observed bottom temperature since 2008 from a bottom-mounted mooring at a location on the inner Scotian Shelf with water depth of 160 m (Figure 1, location 1), from the Atlantic Zone Monitoring Program (AZMP) of Fisheries and Oceans Canada. The mooring is situated on the path of the coastal Nova Scotia Current (Hebert et al., 2023). The mooring is repositioned annually in the fall AZMP survey, hence the data is only available until September 2023 for this study.

Product Reference No.	Product ID & type	Data access	Documentation
1	GLOBAL_MULTIYEAR_PHY_001_030, numerical models	EU Copernicus Marine Service Product (2023) https://doi.org/10.48670/moi-00021	Product User Manual (PUM): Drévillon et al., 2023a Quality Information Document (QUID): Drévillon et al., 2023b Journal article: Lellouche et al., 2021
2	GHRSST Level 4 CMC 0.2 deg global sea surface temperature analysis, 1993-2016	https://doi.org/10.5067/GHCMC-4FM02	Journal article: Brasnett, 2008; CMC 2012
3	GHRSST Level 4 CMC 0.1 deg global sea surface temperature analysis, 2017-2023	https://doi.org/10.5067/GHCMC-4FM03	Journal article: Meissner et al., 2016; CMC 2016
4	Mooring temperature from the AZMP	https://www.dfo-mpo.gc.ca/science/data-donnees/azmp-pmza/index-eng.html	Hebert et al., 2023

Table 1: Product reference table.

2.2 Definition and quantification of marine heatwaves and cold spells

Following Hobday et al., (2016), the MHWs (MCSs) are defined as periods of extremely warm (cold) water that last continuously for five or more days. A seasonally varying climatological percentile threshold method is used to detect MHWs (MCSs). The climatological mean and thresholds (90^{th} and 10^{th} percentiles of data values) are calculated for each day of the year with all data from multiple years within an 11-day window centred on that day. The climatology and thresholds are defined over 30 years from 1993 to 2022 for GLORYS and CMC SST, and from 2010 to 2022 for the mooring observations. A 30-day 'moving window' is applied to smooth the daily climatology. The MHWs and MCSs are defined for temperatures above the 90^{th} and below the 10^{th} percentile values, respectively. Events that occur less than 2 days apart will be considered as one continuous event. The statistics for each MHW (MCS) event are calculated using a Matlab-based tool (Zhao and Marin, 2019).

https://doi.org/10.5194/sp-2024-17
Preprint. Discussion started: 23 September 2024

The mean intensity is the mean SST anomaly during one event. This study is going to focus on the annual statistics of frequency, total days and mean intensity. Frequency refers to the total count of MHW (or MCS) events in each year, while total days are the total number of MHW (or MCS) days in each year. The MHW (or MCS) duration is roughly the total days divided by the frequency.

3 Results

3.1 Spatial distribution of annual surface MHW and MCS parameters

For surface MWHs, GLORYS and CMC SST data obtain overall similar magnitudes and spatial patterns of frequency, total days and mean intensity (Figs. 1a-f). For frequency, values of 1-2 per year on shelf are lower than 2-3 in deep regions beyond the shelf break. In deep regions GLORYS obtains higher frequency than CMC SST. For the total days, GLORYS and CMC SST obtain similar values greater than 30 days per year beyond shelf break in the Scotian Slope and to the east of Labrador Shelf, and over the Grand Banks for Newfoundland (GBN). In the Gulf of Maine, Scotian Shelf, Gulf of St. Lawrence and Labrador Shelf, GLORYS obtains 20-30 days, higher than 20-25 days from CMCSST. For the mean intensity, both GLORYS and CMCSST obtain consistently higher values of 3-6°C in the deep water of Scotian Slope and to the east of southern GBN, and lower values of less than 2.5°C on the shelf and in the deep water to the east of Labrador Shelf.

https://doi.org/10.5194/sp-2024-17
Preprint. Discussion started: 23 September 2024

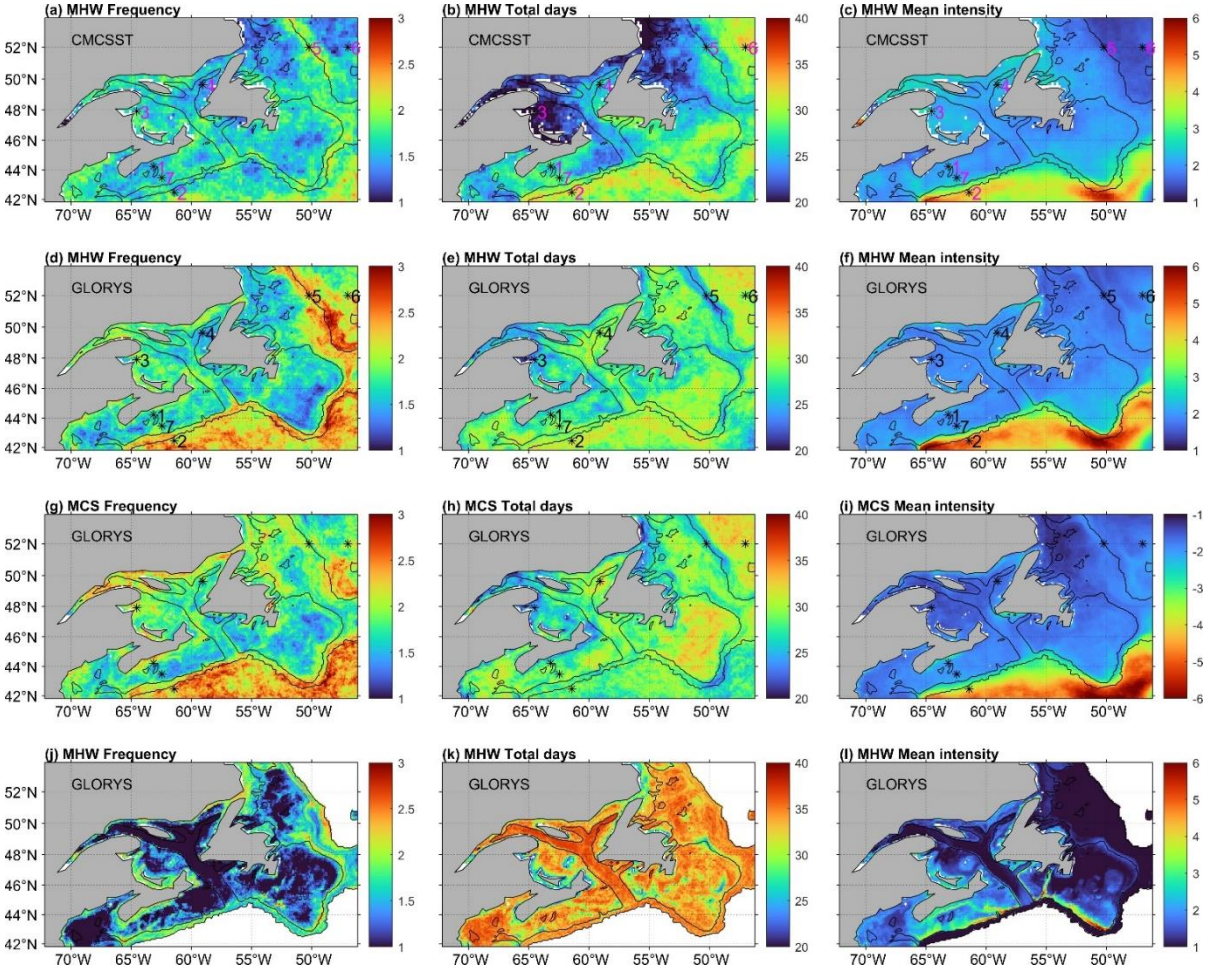

Figure 1: Mean of surface MHW (a-f) and MCS (g-i) characteristics during 1993-2022 derived from (a-c) CMC SST and (d-i) GLORYS. (j-l) Mean of bottom MHW characteristics during 1993-2022 derived from GLORYS. From left to right: frequency, total days, and mean intensity. The black lines represent 200 and 2000 m isobaths. The Halifax line is the line between stations 1 and 2.

https://doi.org/10.5194/sp-2024-17
Preprint. Discussion started: 23 September 2024

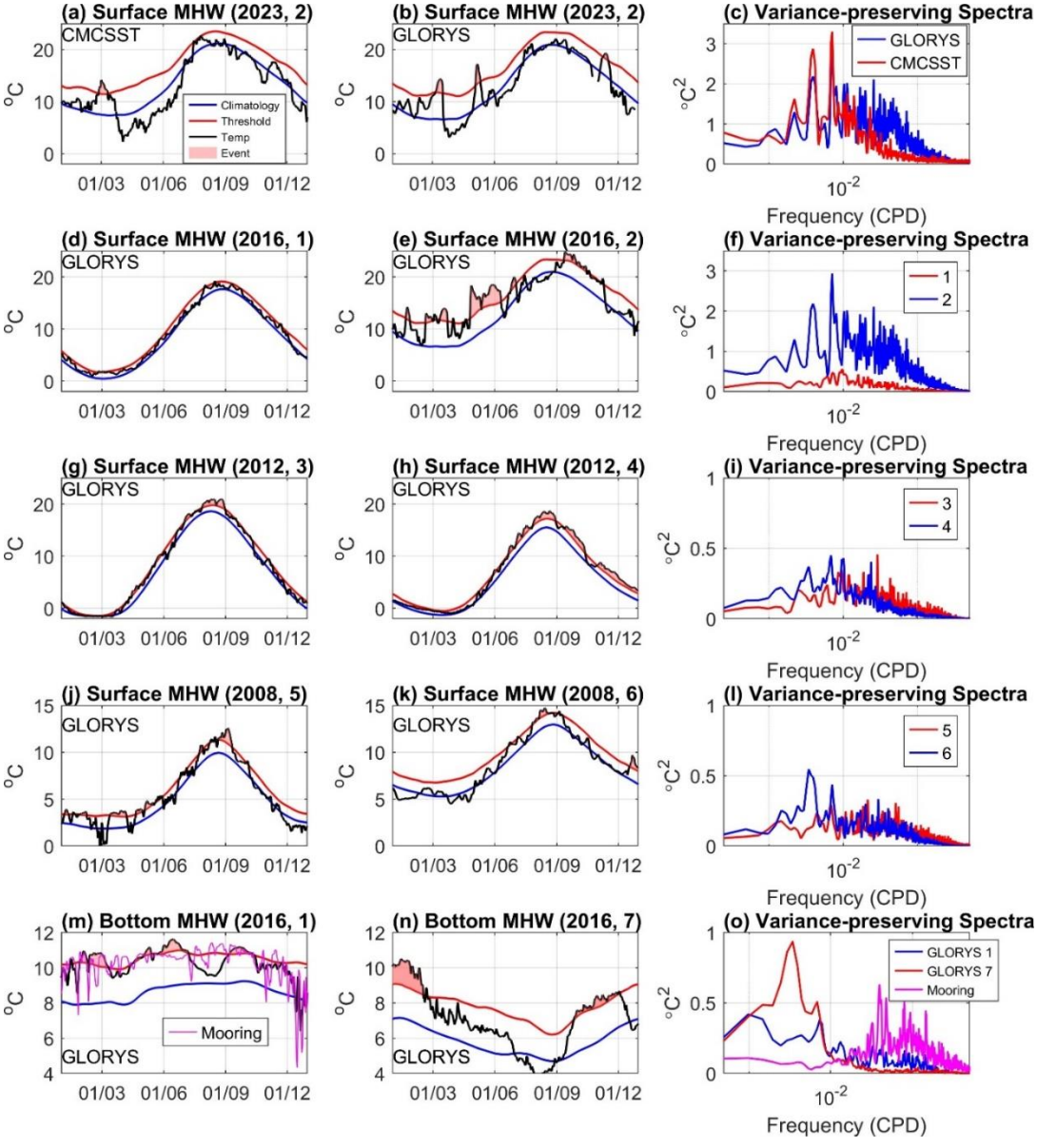

Figure 2: Evolution of MHW at the surface (a, b, d, e, g, h, j, k) and at the seabed (m, n) at 7 locations marked in Figure 1. The numbers in the bracket indicate the year and location. Variance preserving spectra of (c, f, i) surface temperature for the period of 1993 to 2022 and (o) bottom temperature for the period of 2010 to 2022.

The differences between GLORYS and CMC SST in the surface MHW frequency and total days in the Scotian Slope can be explained by their differences in the SST time series (Figs. 2a-b) and variance-preserving spectra (Fig. 2c) at location 2 denoted in Fig. 1. Compared with CMC SST, GLORYS obtains more frequent and stronger temperature variations, and higher spectral power at time scales less than 50 days. For instance, in 2023, GLORYS detected three shorter MHW events

https://doi.org/10.5194/sp-2024-17
Preprint. Discussion started: 23 September 2024

whereas CMC SST detected one longer MHW event (Figs. 2a-b). The differences can be attributed to the interpolations applied in generating the CMC SST. In the southern and western Gulf of St Lawrence, the St. Lawrence Estuary and on the Labrador Shelf, CMC SST obtains shorter total days than GLORYS. This can be attributed to the missing data in CMC SST due to the presence of sea ice in these regions.

The spatial patterns of MHW parameters from GLORYS (Figs. 1d-f) are explained next. The differences between the shelf and the Scotian Slope are demonstrated by comparing the time series and spectra at locations 1 and 2 (Figs. 2d-f). At all the time scales, location 2 shows much stronger SST variability. In 2016, GLORYS detected 6 strong MHW events at location 2 while only one weak event at location 1. In the Gulf of St. Lawrence (GSL), the average annual frequency (Fig. 1d) is lower in the northeastern and higher in the southwestern parts, while the total days (Fig. 1e) show the opposite pattern. At locations 3 and 4, the SST time series in 2012 are similar (Figs. 2g-h). The spectral energy (Fig. 2i) at location 3 is higher at time scales shorter than 100 days hence leading to higher MHW frequency, and at location 4 is higher at time scales longer than 100 days hence leading to higher total days. Off the Labrador Shelf, over a narrow zone nearby the 2000 m isobath, the surface MHW frequency is higher while the total days is shorter, compared to shelf water to the west and the deep water to the east. This again can be explained by the stronger SST variability at time scales shorter than 100 days at location 5 and longer than 100 days at location 6, respectively (Figs. 2j-l). Location 5 is along the path of the offshore Labrador Current, where the SST anomalies and seasonal cycle are both strong, which can be attributed to the variations of temperature front in this area (e.g., Lu et al., 2006).

For the surface MCSs, their frequency, total days and mean intensity (Figs. 1g-i) show similar magnitudes and spatial distribution with those of surface MHWs (Figs. 1d-f). Differences are evident in some areas, e.g., in the Scotian Slope (near location 2) the MHWs have lower frequency and higher mean intensity than the MCSs. These similarities and differences can be explained by the probability distribution of SST anomalies at representative sites shown in Fig. A1. The normalized histograms are nearly symmetrical around the mean, with equal median and mean values. At location 2 the median value is less than the mean, suggesting a positive skewness of SST anomalies in the Scotian Slope due to the dominance of warm-core eddies at the poleward side of the Gulf Stream (e.g., Thompson and Demirov, 2006). Such asymmetric distribution of SST anomalies corresponds to stronger MHWs than MCSs (Schlegel et al., 2021a; Wang et al., 2022).

3.2 Distribution of MHW parameters over the sea floor and in the water column

The frequency, total days and mean intensity of bottom MHWs on the shelf derived from GLORYS (Figs. 1j-l) show different magnitudes and spatial distributions compared to surface MHWs. Our findings are consistent with Amaya et al., (2023) who showed that bottom MHW intensity and duration vary strongly with bottom depth. The bottom MHW frequency (Fig. 1j) shows fewer events (< 1) in deep basins and channels, and more events (2-3) along the coast and shelf break. The bottom MHW total days (Fig. 1k) exhibit weak spatial variations across the entire region with values of 30-35 days, and larger values in deeper basins and channels than in shallow waters. This implies that the bottom MHW durations (roughly total days

https://doi.org/10.5194/sp-2024-17
Preprint. Discussion started: 23 September 2024

divided by frequency) are longer in deep basins and channels than in shallow water. The bottom MHWs intensity (Fig. 1l) ranges from 1°C in deeper parts of the continental shelves to 6°C along the edges of the Scotian Shelf and southern GBN where water intrusions from the shelf break occur.

We selected two locations on the Scotian Shelf to illustrate the difference in MCS characteristics at the sea floor (Figs. 2m-o). Location 1 is the mooring site near the coast where the water depth is 160 m, and location 7 is on the Emerald Bank in the middle of the Scotian Shelf where the water depth is 66 m. At location 1, both GLORYS and mooring observations (Fig. 2m) show that bottom temperatures in 2016 were generally above the mean climatology and extreme heat events were detected throughout the year. However, mooring data show some intense cold spikes that are not captured by GLORYS. Correspondingly, compared with the mooring data, the spectral energy of GLORYS is lower at time scales shorter than 100 days and higher energy at longer than 100 days (Fig. 2o). At location 7, GLORYS detected two MHW events with longer durations in 2016 (Fig.2n). The power spectra of two locations (Fig.2o) show that location 1 has more energy at time scales lower than 100 days, corresponding to higher MHW frequency and mean intensity, while location 7 shows stronger variability at time scales longer than 100 days, corresponding to longer MHW duration and lower intensity. The strong variations of bottom temperature at shorter than 100 days at location 1 are likely related to the strong fluctuations of the coastal Nova Scotia Current driven by local winds at synoptic scales (Dever et al., 2016).

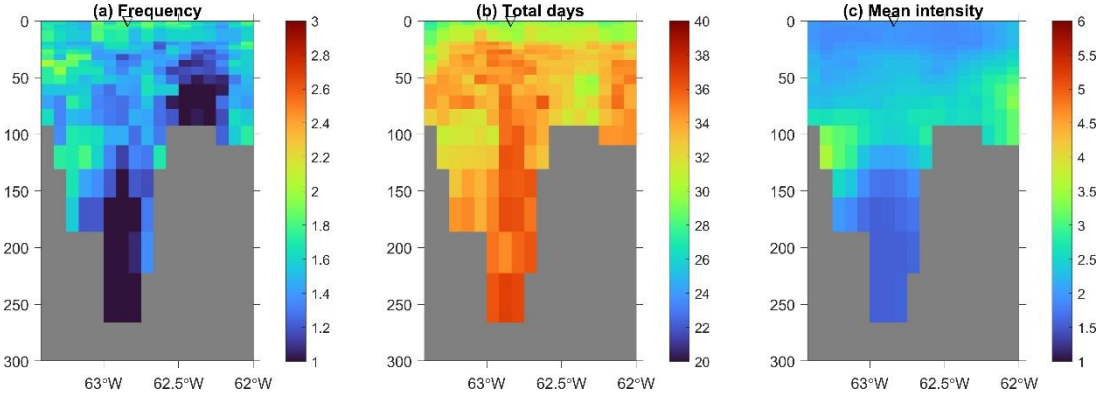

https://doi.org/10.5194/sp-2024-17
Preprint. Discussion started: 23 September 2024

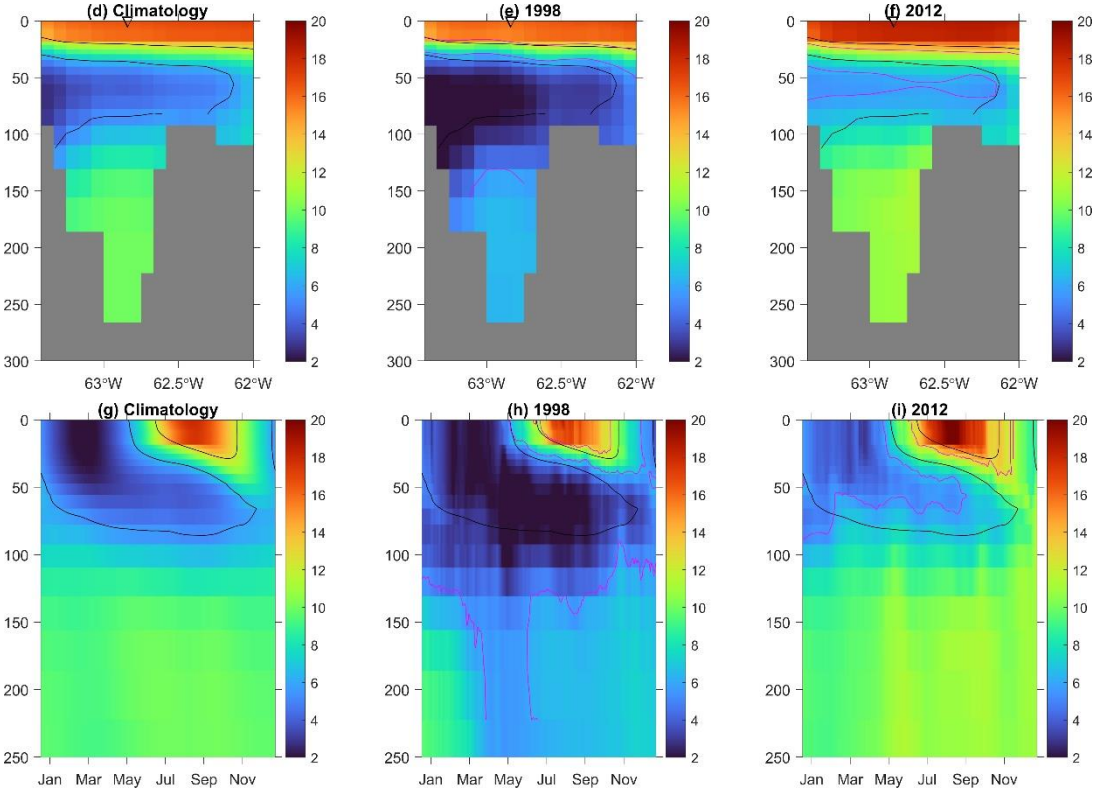

Figure 3: (a-c) MHW mean annual frequency, mean of annual total days, and mean intensity along the Halifax line (a line between stations 1 and 2), (d-f) summer (July-September) temperature along the Halifax line, and (g-i) temperature evolution at a station (marked by a black triangle) along the Halifax line. (d, g) climatology averaged over 1993-2022. Temperature in 1998 (e, h) and 2012 (f, i). The isotherms of 6 and 12 °C averaged over 1993-2022, and in 1998 and 2012 are denoted with black and magenta curves, respectively.

Figures 3a-c present the distributions of MHW parameters in the water column along a section extending off the coast from Halifax between stations 1 and 2 (marked in Fig. 1). The MHW mean intensity shows a clear 3-layer structure, with values of about 2ºC in the upper layer from surface to a mid-depth interface (decreasing from about 70 m near the coast to about 30 m on the Emerald Bank), high values of 3-3.5ºC in the middle layer from the mid-depth interface to about 130 m, and low values of 1.5-2ºC below 130 m depth in the Emerald Basin. The annual NHW frequency is relatively unform in the water column with values 1.5-2, except low values (<1) below 130 m depth in the Emerald Basin and below 30 m depth over the Emerald Bank where the annual MHW duration is high.

The distribution of MHW parameters in the water column can be explained by the layered structure of temperature along this section in summer (Figs. 3d-f) and the seasonal evolution of the vertical profiles of temperature at a location in the middle of Emerald Basin (Figs. 3g-i), for the mean climatology and in 1998 and 2012, respectively. The upper layer (from surface to the mid-depth interface) shows strong seasonal variations. This layer is well mixed in fall/winter, and has strong stratification developed from spring to summer. Seasonal and interannual variations in this upper layer are mainly due to variations of the surface heat flux, and near the coast are also influenced by variations in the Gulf of St. Lawrence which are

https://doi.org/10.5194/sp-2024-17
Preprint. Discussion started: 23 September 2024

also mainly driven by the surface flux (Umoh and Thompson, 1994; Dever et al., 2016). The overall major influence of surface heat flux results in a nearly uniform distribution of the MHW parameters in the upper layer. The middle layer (from the mid-depth interface to about 130 m depth) presents moderate seasonal variations which can be related to the downward penetration of the upper layer driven by surface winds and mixing. On the other hand, this layer is also influenced by the later advection of water masses, mainly from the Cabot Strait subsurface water (30-50 m) and the warm Scotian Slope water and with a smaller portion from the Cabot Strait cold-intermediate layer (50-120 m) and the inshore Labrador Current (Dever et al., 2016). The contributions of the lateral advection vary from the coast to offshore, resulting to the horizontal transition of the depth-range of mid-depth layer from near the coast to the Emerald Bank. The influences of surface forcing and horizontal advection cause high MHW intensity across the whole mid-depth layer, and the low MHW frequency over the Emerald Bank. The deep layer below 130 m depth in the Emerald Basin presents weak seasonal variations but strong interannual variations (Figs. 3g-i). The temperature variations in this deep layer are mainly caused by the intrusion of the offshore water (Dever et al., 2016), leading to low MHW intensity and frequency, and long durations.

3.3 Interannual variations of MHW/MCS parameters

Interannual variations of the MHW/MCS parameters at location 1 in the inner Scotian Shelf are presented in Fig. 4, and some of their statistical quantifications are summarized in Table 2. For the surface parameters, variations of their values derived from GLORYS have high correlations with those derived from CMC SST except for the MCS mean intensity. The surface MHW (MCS) frequency and total days show strong interannual variations which have significantly positive (negative) correlations with the annual SST anomalies from GLORYS. The MHW/MCS mean intensities show weaker interannual variations and have no significant correlations with the SST anomalies.

For the bottom parameters, significant correlation values derived from GLORYS and available mooring data are found for the MHW frequency, total days and mean intensity, but not for the MCS parameters. This can be attributed to GLORYS not being able to reproduce the intense cold spikes in mooring observations (Fig. 2m). For both the bottom MHWs and MCSs, interannual variations of their frequency, total days and mean intensity all have significant correlations with the annual bottom temperature anomalies from GLORYS. The bottom MHW total days and mean intensity derived from the mooring data are significantly lower than those derived from GLORYS. This is due to the differences in the bottom temperature climatology of the two datasets defined for the calculation of the MHW/MCS parameters. While the two datasets show similar values and increasing trends in the bottom temperatures, the climatology of mooring data during the recent 16 years of 2008-2023 has a higher level than that of GLORYS during 30 years of 1993-2022. As a result, the mooring data obtains shorter and weaker bottom MHW events than GLORYS.

At location 1 during 1993-2023, both at surface and bottom, interannual variations of the MHW and MCS total days are negatively correlated; the intensity and total days of MHWs show positive trends, while those for MCSs show negative trends. These correspond to warming trends in both the SST and bottom temperature (Figs. 4i-j). The MHW and MCS mean intensities show no significant trends at surface, but positive trends at bottom. For the bottom MHW/MCS total days, the trends

https://doi.org/10.5194/sp-2024-17
Preprint. Discussion started: 23 September 2024

are mostly due to their sharp increases (or regime shift) around 2012 (Figs. 4b & f). Out of the 19 years before 2012, bottom MCS events are detected in 11 years while MHW events are detected only in 2 years. By comparison, out of the 12 years since 2012, bottom MHW events are detected in 10 years while MCS events are detected only in one year. These correspond to the sharp increase of bottom temperature that also occurred around 2012 (Fig. 4j). By comparison, the SST at location 1 shows a more gradual increasing trend (Fig. 4i). After 2012, the annual bottom temperature became higher than the annual SST. As a result, the bottom MHW total days frequently exceeded 200, higher than 50-70 for large values of the surface MHW total days (Figs. 4a & b). The long-term trends and regime shifts of bottom MHW/MCS total days are wide spread on the Scotian Shelf, as evidenced by the similar time series as location 1 at a location in the Emerald Basin and location 7 on the Emerald Shelf (Fig. A2).

The time series plots identify years when severe MHW or MCS events occurred. At location 1, the surface MHW total days show the highest values in 2012, reaching 215 days according to GLORYS. Both GLORYS and CMC SST detect 7 MHW events and each one lasted 7 to 61 days. These prolonged surface MHW events correspond to the highest peak of annual SST (Fig. 4i) and the well-known warming condition across the Scotian Shelf (Hebert et al., 2013) and in the Gulf of Maine and the east coast of the USA in 2012 (Chen et al., 2015). In December 2011 the SST in the region was close to the 90th percentile and likely played a role in preconditioning the MHW in January 2012. Chen et al. (2015) further attributed the widespread MHW events to persistent atmospheric high-pressure systems featured by anomalously weak wind speeds, increased insolation, and reduced ocean heat losses. At location 1, the termination of a long-lasting and strong surface MHW event in the summer of 2012 (Fig. 3i) can be attributed to wind-induced coastal upwelling, resulting in a sudden drop in SST at the end of August (Shan and Sheng, 2022).

In 2012 at location 1, the bottom MHW total days experienced a sharp increase relative to previous years, reaching ~100 days according to GLORYS (Fig.4b). In the summer of 2012, the entire water column along the Halifax Line was warmer than the climatology (Figs. 3d & f). In the Emerald Basin (Figs. 3g & i), the abnormally warm condition presented from surface to about 100 m depth at the beginning of the year (winter), which can be attributed to the smaller heat loss to the atmosphere at the sea surface. Below the 100 m depth, warming started in spring. Below the upper layer directly influenced by surface forcing, the warming in 2012 can be attributed to the advection of abnormally warm Scotian Slope water combined with the reduced contribution of the cold water from the Gulf of St Lawrence or the inner Labrador Shelf (Dever et al., 2016). The warm Scotian Slope water was influenced by the interaction between the Gulf Stream and the Labrador Current at the tail of the Grand Banks of Newfoundland) (Brickman et al., 2018).

The condition in 1998 is opposite to that in 2012, i.e., 1) location 1 experienced the longest bottom MCS total days (nearly 300 days) associated with the lowest annual bottom temperature value (Figs. 4f & j); 2) in summer the entire water column along the Halifax Line was colder than the climatology (Figs. 3d & e); and 3) in the Emerald Basin (Figs. 3g & h) the entire water column was enormously cold throughout the year except for close to normal condition in the upper layer in summer. Below 150 m depth in the Emerald Basin, the lowest temperature occurred during March-June. This can be related

https://doi.org/10.5194/sp-2024-17
Preprint. Discussion started: 23 September 2024

277 to the intrusion of the cold Labrador Slope water. According to Drinkwater et al. (2003), this cold water mass was advected
278 along the shelf break in 1997-1998 and flooded the lower layers of the central and southwestern regions of the Scotian Shelf.
279 In 2023, according to GLORYS, the MHW total days is 85, which is well above the average value of 31 days. The
280 mean intensity was 2°C, similar to the normal intensity. The longest MHW event of that year began on December 19, 2022,
281 and continued until February 8, 2023, coinciding with the warmest January on record in Halifax. The termination of this MHW
282 event is likely related to an extremely cold Arctic air outbreak that set many local meteorological records in early February in
283 Atlantic Canada and caused rapid drops of water temperature in some shallow coastal bays (Casey et al., 2024).
284

https://doi.org/10.5194/sp-2024-17
Preprint. Discussion started: 23 September 2024

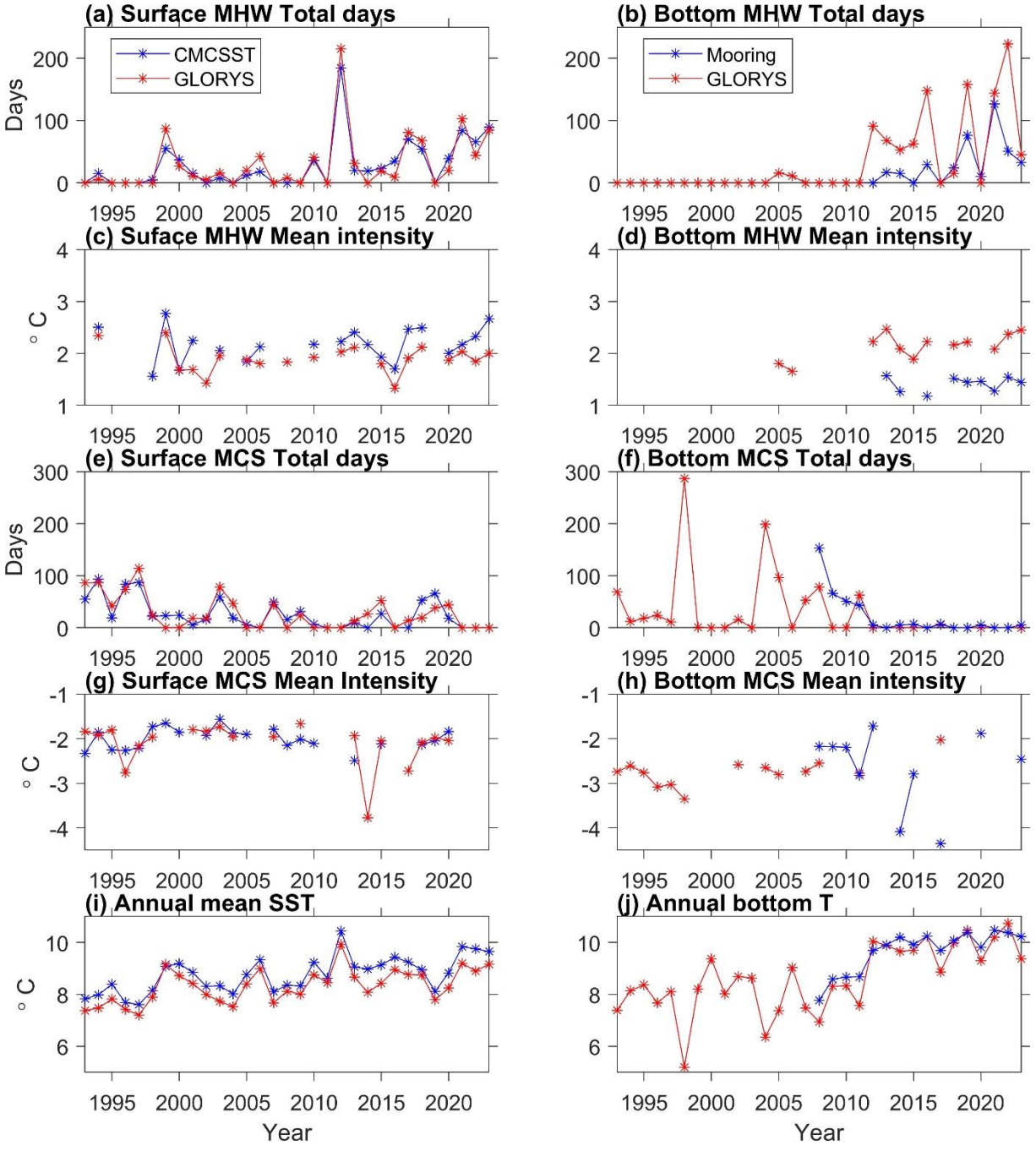

Figure 4: Time series of MHW and MCS characteristics at location 1 (marked in Fig. 1). Left for surface & right for bottom. Row 1: MHW total day; row 2: MHW mean intensity; row 3: MCS total days; row 4: MCS intensity; row 5: Comparison of annual mean time series of GLORYS with CMCSST and mooring observations.

https://doi.org/10.5194/sp-2024-17
Preprint. Discussion started: 23 September 2024

	Trend	Correlation with obs	Correlation with T
Surface			
MHW frequency	0.07	0.83	0.86
MHW total day	1.9	0.96	0.81
MHW intensity	-	0.77	-
MCS frequency	-0.1	0.69	-0.8
MCS total day	-1.8	0.84	-0.81
MCS intensity	-	-	-
Bottom			
MHW frequency	0.2	0.77	0.72
MHW total day	4.1	0.75	0.7
MHW intensity	0.03	0.64	0.59
MCS frequency	-0.1	-	-0.75
MCS total day	-2.3	-	-0.78
MCS intensity	0.03	-	0.59

Table 2: Statistics of annual values of MHW/MCS parameters during 1993-2023 at location 1 on the inner Scotian Shelf. Column 2: linear trends of MHW/MCS frequency in events/year, total days in days/year, and mean intensity in °C/year derived from GLORYS. Column 3: correlation coefficient of MHW/MCS parameters derived from GLORYS and observed temperature. Column 4: correlation coefficient between MHW/MCS parameters and annual GLORYS temperature. Significant trends and correlations with p-values less than 0.1 are shown.

4 Conclusions and discussions

First, in this study the MWH/MCS parameters derived from GLORYS and observational data are compared. At surface, GLORYS and CMC SST obtain similar magnitudes, spatial distribution and interannual variations of MHW/MCS frequency, total days and mean intensity. Differences in the values of the parameters can be attributed to issues in the CMC SST data: 1) shorter MHW total days in the Gulf of St. Lawrence and Labrador Shelf due to the missing SST data in the presence of ice, and 2) less frequent MHWs in the deep Scotian Slope associated with weaker SST variations caused by the interpolations and cloud correction applied to the satellite remote sensing data for generating the CMC SST. Thus, we suggest that high-resolution data assimilative ocean reanalysis products possess more advantages in quantifying surface MHWs and MCSs than SST products based on satellite remote sensing. For the bottom MHWs and MCSs, the analysis results from

https://doi.org/10.5194/sp-2024-17
Preprint. Discussion started: 23 September 2024

GLORYS are compared with those from 16 years of bottom mooring observations at location 1 near the coast of Nova Scotia. GLORYS does not reproduce the intense cold spikes of observed bottom temperature hence potentially detect less bottom MCSs at this location strongly influenced by the variations of Nova Scotia Current. GLORYS well reproduces the observed rising trend and sharp increase of bottom temperature around 2012 on Scotian Shelf. The 31 years (1993-2023) of GLORYS data enables the quantification of spatial variations, interannual variations and long-term trends of the water column and bottom MHW/MCS parameters for the first time in our study region.

Second, the horizontal/depth distributions of annual MHW/MCS parameters are explained by the characteristics of temperature variations and the related ocean dynamics. The corresponding parameters of surface MHWs and MCSs are overall similar due to the nearly symmetrical probability distribution of SST anomalies around the mean, except in the Scotian Slope where the MHWs have lower frequency and higher mean intensity than the MCSs due to the dominance of warm-core eddies. The surface MHWs have the highest frequency (2-3 per year) and mean intensity (3-6°C) in the Scotian Slope and to the east of southern GBN, due to the strong SST variability associated with the eddy activities and variations of Gulf Stream and North Atlantic Current. The shelf waters show nearly uniform values of the surface MHW parameters: 1-2 per year for frequency, 20-30 days per year for total days, and ~2.0°C for the mean intensity. The bottom MHW frequency, duration (approximately total days divided by frequency) and mean intensity vary strongly with bottom depth, which can be explained by the layered structure of MHW parameters and temperature along a cross-shelf section off Halifax (Fig.3). In the upper layer from surface to a mid-depth interface, the nearly uniform MHW mean intensity of ~2ºC can be mainly attributed to variations of the surface heat flux. From the mid-depth interface to about 130 m depth, the MHW mean intensity has high values of 3-3.5ºC which can be related to the combined effects of downward penetration of upper layer (through wind forcing and mixing) and the lateral advection of water masses from the Cabot Strait subsurface and cold-intermediate layers, the Scotian Slope water and the inshore Labrador Current. In the deep Emerald Basin below 130 m depth, the MHW intensity has the lowest values of 1.5-2ºC due to intrusions of offshore water. The MHW frequency has relatively unform values of 1.5-2 per year in the water column, except low values of less than 1 per year (corresponding to longer MHW durations) below 130 m depth in the Emerald Basin and below 30 m depth over the Emerald Bank. This can be attributed to the different characteristics of temperature variations caused by different forcings: stronger variations at shorter (longer) time scales by surfacing forcing (lateral intrusion).

Thirdly, analysis of the GLORYS data reveals interannual variations, long-term trends and regime shifts of MHW/MCS parameters during 1993-2023. For the surface MHW (MCS) total days, 1) their annual values have significantly positive (negative) correlations with the annual SST anomalies; 2) their increasing (decreasing) trends correspond to the gradual increasing SST; and 3) the peak value (215 days) of MHW total days in 2012 corresponds to the highest annual SST representing the well-known warming condition across the Scotian Shelf, Gulf of Maine and the east coast of the USA. The bottom temperature shows a stronger increasing trend than the SST, and a sharp increase (regime shift) around 2012. This causes the increasing (decreasing) trend and regime shift of MHW (MCS) total days. After 2012 at location 1, the annual bottom temperature became higher than the annual SST; and the bottom MHW total days frequently exceeded 200, higher than 50-70 for large values of the surface MHW total days. In 2012, the bottom MHW total days at location 1 experienced a sharp

https://doi.org/10.5194/sp-2024-17
Preprint. Discussion started: 23 September 2024

increase to ~100 days; and the entire water column along the Halifax Line was warmer than the climatology due to the smaller heat loss to the atmosphere at the sea surface, the advection of abnormally warm Scotian Slope water, and the reduced contribution of the cold water from the Gulf of St Lawrence or the inner Labrador Shelf. Opposite condition presented in 1998 with the longest bottom MCS total days of ~300 days at location 1, and the entire water column along the Halifax Line was colder than the climatology.

We note that the detection of MHWs and MCSs and the quantification of their parameters depend on the reference climatology of ocean temperature, in particularly in our study region with evident warming trends over the past several decades. Defining the climatology over 30 years (1993-2022) with the GLORYS data obtains longer total days and stronger intensity for bottom MHWs, compared with using the recent 16 years (2008-2023) of bottom temperature from mooring observations. There are ongoing debates in the literature about whether the long-term trends in ocean temperature should be included or excluded in MHW research (Oliver et al., 2021; Zhang et al., 2024). Amaya et al., (2023) proposed that both approaches could be useful depending on the applications of interest. The long-term warming trends and short-duration extreme events likely cause different physiological and behavioural responses of marine species. In the present study, the long-term warming trend is retained in defining the water temperature climatology and the detection of MHWs and MCSs, while in the future we may consider to exclude the trends when investigating the impacts of MHWs and MCSs on marine ecosystems and fisheries.

Previous studies have revealed the linkage of the declining North Atlantic right whale population to the significant warming in the Gulf of Maine and the western Scotian Shelf over the recent decades (Meyer-Gutbrod et al., 2021), and the impacts of the extreme cold (warm) event in 1998 (2012) on certain fishery species. In 1998, shortly after the cold Labrador Slope Water replaced the Warm Slope Water, the catches of porbeagle shark and silver hake in the Emerald Basin dramatically declined (Drinkwater et al., 2002). In 2012, the anomalously warm bottom water had opposite effects on lobster and snow crab fisheries (Mills et al., 2013; Zisserson and Cook, 2017). We plan more studies of such nature in the Northwest Atlantic using the GLORYS reanalysis product validated with observational data such as from the AZMP survey.

Data and code availability

The data used in this study are available as described in Table 1. The code used in this study can be accessed via a GitLab repository upon request via email to the corresponding author.

Author contribution

LZ and YL led the conceptualization of the study, analysis and writing of the manuscript. HW refined the scripts of data analysis. GG and SVG contributed to the conceptualization of the study, and editing and reviewing the manuscript.

Competing interests

The authors declare that they have no conflict of interest.

https://doi.org/10.5194/sp-2024-17
Preprint. Discussion started: 23 September 2024

Acknowledgments

We appreciate DFO and Mercator-Ocean International for supporting the scientific exchanges and collaboration between the staff of both organizations, in recent years under a collaborative agreement, Dr. David Brickman for commenting on an early version of the manuscript, and Dr. Karina Von Schuckmann for insightful comments and advice in developing this manuscript.

https://doi.org/10.5194/sp-2024-17
Preprint. Discussion started: 23 September 2024

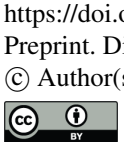

STATE OF THE PLANET Discussions

389 **Appendix:**

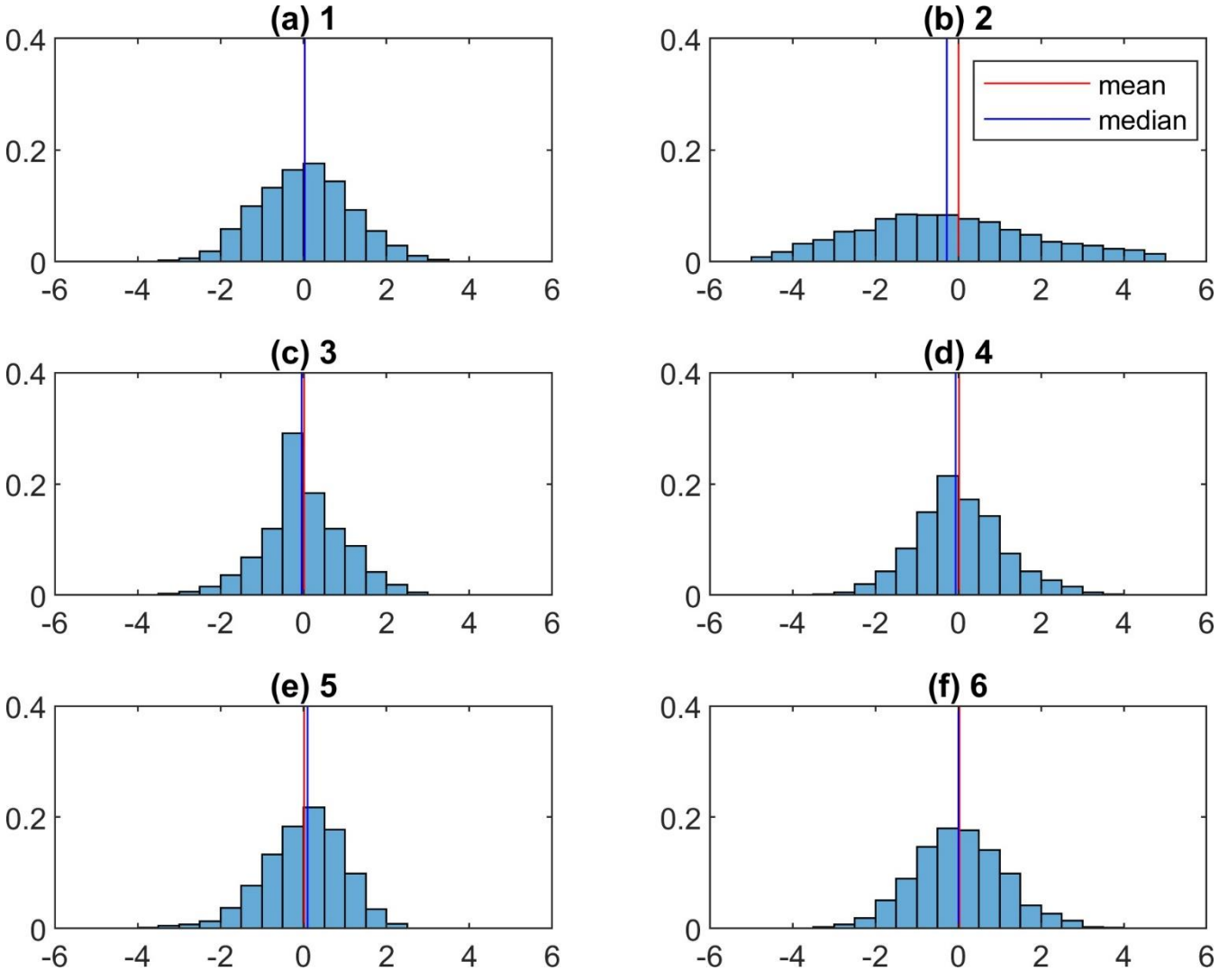

390
391

392 **Figure A1: Histogram of surface temperature anomalies at six locations marked in Fig. 1.**

393

https://doi.org/10.5194/sp-2024-17
Preprint. Discussion started: 23 September 2024

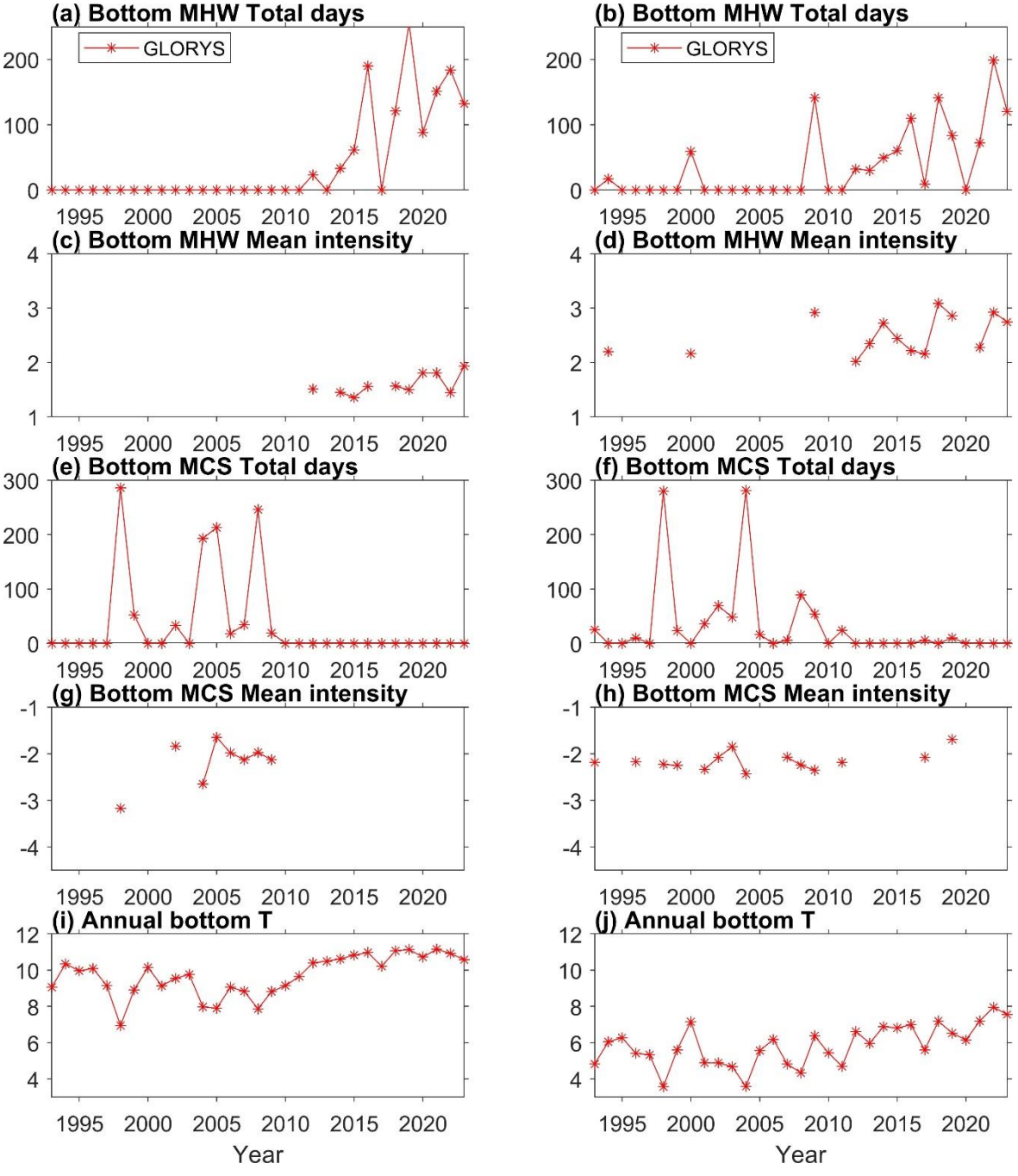

Figure A2. Time series of bottom MHW/MCS paramters and bottom temperature derived from GLORYS at (left column) a location in Emerald Basin (marked as a triangle in Fig. 3a) and (right colum) location 7 on Emerald Bank. The location in Emerald Basin is marked as a triangle in Figure 3a.

https://doi.org/10.5194/sp-2024-17
Preprint. Discussion started: 23 September 2024

References:

Amaya, D.J., Jacox, M.G., Alexander, M.A., Scott, J.D., Deser, C., Capotondi, A., Phillips, A.S., 2023. Bottom marine heatwaves along the continental shelves of North America. Nat. Commun. 14, 1038. https://doi.org/10.1038/s41467-023-36567-0

Amaya, D.J., Jacox, M.G., Fewings, M.R., Saba, V.S., Stuecker, M.F., Rykaczewski, R.R., Ross, A.C., Stock, C.A., Capotondi, A., Petrik, C.M., Bograd, S.J., Alexander, M.A., Cheng, W., Hermann, A.J., Kearney, K.A., Powell, B.S., 2023. Marine heatwaves need clear definitions so coastal communities can adapt. Nature 616, 29–32. https://doi.org/10.1038/d41586-023-00924-2

Brasnett, B., 2008. The impact of satellite retrievals in a global sea-surface-temperature analysis. Q. J. R. Meteorol. Soc. 134, 1745–1760. https://doi.org/10.1002/qj.319

Brickman, D., Hebert, D., Wang, Z., 2018. Mechanism for the recent ocean warming events on the Scotian Shelf of eastern Canada. Cont. Shelf Res. 156, 11–22. https://doi.org/10.1016/j.csr.2018.01.001

Canada Meteorological Center. 2012. CMC 0.2 deg global sea surface temperature analysis. Ver. 2.0. PO.DAAC, CA, USA. Dataset accessed [YYYY-MM-DD] at https://doi.org/10.5067/GHCMC-4FM02

Canada Meteorological Center. 2016. GHRSST Level 4 CMC 0.1 deg global sea surface temperature analysis. Ver. 3.0. PO.DAAC, CA, USA. Dataset accessed [YYYY-MM-DD] at https://doi.org/10.5067/GHCMC-4FM03

Dever, M., Hebert, D., Greenan, B.J.W., Sheng, J., Smith, P.C., 2016. Hydrography and Coastal Circulation along the Halifax Line and the Connections with the Gulf of St. Lawrence. Atmosphere-Ocean 54, 199–217. https://doi.org/10.1080/07055900.2016.1189397

DFO, 2003. 2001 State of the Ocean: Physical Oceanographic Conditions on the Scotian Shelf, Bay of Fundy and Gulf of Maine. DFO Science Ecosystem Status Report 2003/002.

Drévillon, M., Fernandez, E., Lellouche, J.M.: EU Copernicus Marine Service Product User Manual for the Global Ocean Physics Reanalysis, GLOBAL_MULTIYEAR_PHY_001_030, Issue 1.5, Mercator Ocean International, https://catalogue.marine.copernicus.eu/documents/PUM/CMEMS-GLO-PUM-001-030.pdf, last access: 19 March 2024, 2023

Drévillon, M., Lellouche, J.M., Régnier, C., Garric, G., Bricaud, C., Hernandez, O., and Bourdallé-Badie, R.: EU Copernicus Marine Service Quality Information Document for the Global Ocean Physics Reanalysis, GLOBAL_MULTIYEAR_PHY_001_030, Issue 1.6, Mercator Ocean International, https://catalogue.marine.copernicus.eu/documents/QUID/CMEMS-GLO-QUID-001-030.pdf, last access: 19 March 2024, 2023

Drinkwater, K.F., Petrie, B., Smith, P.C., 2003. Climate variability on the Scotian Shelf during the 1990s (report). ICES MSS Vol.219 - Hydrobiological variability in the ICES Area, 1990-1999. https://doi.org/10.17895/ices.pub.19271735.v1

Fiedler, E.K., McLaren, A., Banzon, V., Brasnett, B., Ishizaki, S., Kennedy, J., Rayner, N., Roberts-Jones, J., Corlett, G., Merchant, C.J., Donlon, C., 2019. Intercomparison of long-term sea surface temperature analyses using the GHRSST Multi-Product Ensemble (GMPE) system. Remote Sens. Environ. 222, 18–33. https://doi.org/10.1016/j.rse.2018.12.015

Fox-Kemper, B., Hewitt, H.T., Xiao, C., Aðalgeirsdóttir, G., Drijfhout, S.S., Edwards, T.L., Golledge, N.R., Hemer, M., Kopp, R.E., Krinner, G., Mix, A., Notz, D., Nowicki, S., Nurhati, I.S., Ruiz, L., Sallée, J.-B., Slangen, A.B.A., Yu, Y., 2021. Ocean, Cryosphere and Sea Level Change Supplementary Material. Clim. Change 2021 Phys. Sci. Basis Contrib. Work. Group Sixth Assess. Rep. Intergov. Panel Clim. Change.

Free, C.M., Anderson, S.C., Hellmers, E.A., Muhling, B.A., Navarro, M.O., Richerson, K., Rogers, L.A., Satterthwaite, W.H., Thompson, A.R., Burt, J.M., Gaines, S.D., Marshall, K.N., White, J.W., Bellquist, L.F., 2023. Impact of the 2014–2016 marine heatwave on US and Canada West Coast fisheries: Surprises and lessons from key case studies. Fish Fish. 24, 652–674. https://doi.org/10.1111/faf.12753Frölicher, T.L., Fischer, E.M., Gruber, N., 2018. Marine heatwaves under global warming. Nature 560, 360–364. https://doi.org/10.1038/s41586-018-0383-9

Hebert, D., Layton, C., Brickman, D., and Galbraith, P.S. 2023. Physical Oceanographic Conditions on the Scotian Shelf and in the Gulf of Maine during 2022. Can. Tech. Rep. Hydrogr. Ocean Sci. 359: vi + 81 p.

Hobday, A.J., Alexander, L.V., Perkins, S.E., Smale, D.A., Straub, S.C., Oliver, E.C.J., Benthuysen, J.A., Burrows, M.T., Donat, M.G., Feng, M., Holbrook, N.J., Moore, P.J., Scannell, H.A., Sen Gupta, A., Wernberg, T., 2016. A

https://doi.org/10.5194/sp-2024-17
Preprint. Discussion started: 23 September 2024

hierarchical approach to defining marine heatwaves. Prog. Oceanogr. 141, 227–238. https://doi.org/10.1016/j.pocean.2015.12.014

Holbrook, N.J., Scannell, H.A., Sen Gupta, A., Benthuysen, J.A., Feng, M., Oliver, E.C.J., Alexander, L.V., Burrows, M.T., Donat, M.G., Hobday, A.J., Moore, P.J., Perkins-Kirkpatrick, S.E., Smale, D.A., Straub, S.C., Wernberg, T., 2019. A global assessment of marine heatwaves and their drivers. Nat. Commun. 10, 2624. https://doi.org/10.1038/s41467-019-10206-z

Lellouche, J. M., Greiner, E., Bourdallé-Badie, R., Garric, G., Melet. A., Drévillon, M., et al. (2021). The Copernicus Global 1/12° Oceanic and Sea Ice GLORYS12 Reanalysis. Front. Earth Sc-Switz. 9, 698876. doi: 10.3389/feart.2021.698876

Lu, Y., Wright, D. G., Clarke, R.A. 2006: Modelling deep seasonal temperature changes in the Labrador Sea. Geophysical Research Letters, 33, L23601, doi:10.1029/2006GL027692.

Meissner, F. J. Wentz, J. Scott and J. Vazquez-Cuervo,. 2016. Sensitivity of Ocean Surface Salinity Measurements From Spaceborne L-Band Radiometers to Ancillary Sea Surface Temperature, IEEE Transactions on Geoscience and Remote Sensing, 54, 12. https://doi.org/10.1109/TGRS.2016.2596100

Meyer-Gutbrod, E. L., C. H. Greene, K. T. Davies, and D. G. Johns. 2021. Ocean regime shift is driving the collapse of the North Atlantic right whale population. Oceanography 34: 22–31. doi:10.5670/oceanog.2021.308

Mills, K., Pershing, A., Brown, C., Chen, Y., Chiang, F.-S., Holland, D., Lehuta, S., Nye, J., Sun, J., Thomas, A., Wahle, R., 2013. Fisheries Management in a Changing Climate: Lessons From the 2012 Ocean Heat Wave in the Northwest Atlantic. Oceanography 26. https://doi.org/10.5670/oceanog.2013.27

Oliver, E.C.J., Donat, M.G., Burrows, M.T., Moore, P.J., Smale, D.A., Alexander, L.V., Benthuysen, J.A., Feng, M., Sen Gupta, A., Hobday, A.J., Holbrook, N.J., Perkins-Kirkpatrick, S.E., Scannell, H.A., Straub, S.C., Wernberg, T., 2018. Longer and more frequent marine heatwaves over the past century. Nat. Commun. 9, 1324. https://doi.org/10.1038/s41467-018-03732-9

Oliver, E.C.J., Benthuysen, J.A., Darmaraki, S., Donat, M.G., Hobday, A.J., Holbrook, N.J., Schlegel, R.W., Sen Gupta, A., 2021. Marine Heatwaves. Annu. Rev. Mar. Sci. https://doi.org/10.1146/annurev-marine-032720-095144

Santora, J.A., Mantua, N.J., Schroeder, I.D., Field, J.C., Hazen, E.L., Bograd, S.J., Sydeman, W.J., Wells, B.K., Calambokidis, J., Saez, L., Lawson, D., Forney, K.A., 2020. Habitat compression and ecosystem shifts as potential links between marine heatwave and record whale entanglements. Nat. Commun. 11, 536. https://doi.org/10.1038/s41467-019-14215-w

Schlegel, R.W., Darmaraki, S., Benthuysen, J.A., Filbee-Dexter, K., Oliver, E.C.J., 2021a. Marine cold-spells. Prog. Oceanogr. 198, 102684. https://doi.org/10.1016/j.pocean.2021.102684

Schlegel, R.W., Oliver, E.C.J., Chen, K., 2021b. Drivers of Marine Heatwaves in the Northwest Atlantic: The Role of Air–Sea Interaction During Onset and Decline. Front. Mar. Sci. 8, 627970. https://doi.org/10.3389/fmars.2021.627970

Sen Gupta, A., Thomsen, M., Benthuysen, J.A., Hobday, A.J., Oliver, E., Alexander, L.V., Burrows, M.T., Donat, M.G., Feng, M., Holbrook, N.J., Perkins-Kirkpatrick, S., Moore, P.J., Rodrigues, R.R., Scannell, H.A., Taschetto, A.S., Ummenhofer, C.C., Wernberg, T., Smale, D.A., 2020. Drivers and impacts of the most extreme marine heatwave events. Sci. Rep. 10, 19359. https://doi.org/10.1038/s41598-020-75445-3

Shan, S., Sheng, J., 2022. Numerical Study of Topographic Effects on Wind-Driven Coastal Upwelling on the Scotian Shelf. J. Mar. Sci. Eng. 10, 497. https://doi.org/10.3390/jmse10040497

Thompson, K., and E. Demirov (2006), Skewness of sea level variability of the world's oceans, J. Geophys. Res., 111, C05005, doi:10.1029/2004JC002839.

Umoh, J.U., Thompson, K.R., 1994. Surface heat flux, horizontal advection, and the seasonal evolution of water temperature on the Scotian Shelf. J. Geophys. Res. Oceans 99, 20403–20416. https://doi.org/10.1029/94JC01620

Wang, H., Lu, Y., Zhai, L., Chen, X., Liu, S., 2024. Variations of surface marine heatwaves in the Northwest Pacific during 1993–2019. Front. Mar. Sci. 11, 1323702. https://doi.org/10.3389/fmars.2024.1323702

Wang, Y., Kajtar, J.B., Alexander, L.V., Pilo, G.S., Holbrook, N.J., 2022. Understanding the Changing Nature of Marine Cold-Spells. Geophys. Res. Lett. 49, e2021GL097002. https://doi.org/10.1029/2021GL097002

Zhang, M., Cheng, Y., Wang, G., Shu, Q., Zhao, C., Zhang, Y., Qiao, F., 2024. Long-term ocean temperature trend and marine heatwaves. J. Oceanol. Limnol. https://doi.org/10.1007/s00343-023-3160-z

Zhao, Z., Marin, M., 2019. A MATLAB toolbox to detect and analyze marine heatwaves. J. Open Source Softw. 4, 1124. https://doi.org/10.21105/joss.01124

https://doi.org/10.5194/sp-2024-17
Preprint. Discussion started: 23 September 2024

497 Zisserson, B., Cook, A., 2017. Impact of bottom water temperature change on the southernmost snow crab fishery in the
498 Atlantic Ocean. Fish. Res. 195, 12–18. https://doi.org/10.1016/j.fishres.2017.06.009
499